Corrected 12 April 2005; see page 5

Sciencexpress Report

Kinesin and Dynein Move a Peroxisome in Vivo: A Tug-of-War or Coordinated Movement?

Comert Kural,[1] Hwajin Kim,[3] Sheyum Syed,[2] Gohta Goshima,[4] Vladimir I. Gelfand,[3]*† Paul R. Selvin[1,2]‡

[1]Biophysics Center, [2]Physics Department, [3]Department of Cell and Structural Biology, University of Illinois, Urbana, IL 61801, USA. [4]Department of Cellular and Molecular Pharmacology, University of California, San Francisco, CA 94107, USA.

*Present address: Department of Cell and Molecular Biology, Feinberg School of Medicine, Northwestern University, Chicago, IL 60611, USA.

†To whom correspondence should be addressed. Department of Cell and Molecular Biology, Northwestern University School of Medicine, 303 East Chicago Avenue, Ward 11-080, Chicago, IL 60611–3008, USA. E-mail: vgelfand@northwestern.edu

‡To whom correspondence should be addressed. Loomis Lab of Physics, 1110 West Green Street, University of Illinois, Urbana, IL 61801, USA. E-mail: selvin@uiuc.edu

We have used Fluorescence Imaging with One Nanometer Accuracy (FIONA) for analysis of organelle movement by conventional kinesin and cytoplasmic dynein in a cell. We can locate a green fluorescence protein (GFP)–tagged peroxisome in cultured *Drosophila* S2 cells to within 1.5 nanometers in 1.1 milliseconds, a 400-fold improvement in temporal resolution, sufficient to determine the average step size to be ~8 nanometers for both dynein and kinesin. Furthermore, we find that dynein and kinesin do not work against each other in vivo during peroxisome transport. Rather, we find that multiple kinesins or multiple dyneins work together, producing up to 10 times the in vitro speed.

Cytoplasmic kinesin and dynein are microtubule dependent molecular motors responsible for organelle trafficking and cell division. The long-distance organelle transport within a cell occurs bi-directionally along the microtubule tracks. (+) end directed kinesins carry the cargo to the cell periphery whereas (-) end directed dyneins bring the cargo back.

In vitro studies using optical traps (reviewed in (*1*)) and single molecule fluorescence (*2*) have provided insight into how the microtubule motors work. Kinesin is a highly processive motor that can take hundreds of 8 nm steps, with load of up to 6 pN, before detaching from the microtubule (*3*). Optical trap and *in vitro* motility studies have shown that a dynein/dynactin complex is also processive (*4*), and that dynein has an 8 nm step-size under a load of up to 1.1 pN (*5*).

These studies, however, do not address how kinesin and dynein cooperate to achieve intracellular bi-directional transport. Do they move a cargo by a tug-of-war, or is there a switch which turns off one or both of the motors? Do multiple motors of the same polarity act together or cooperatively? (*6*–*8*). Answering these questions requires watching the cargo molecules *in vivo* with high temporal and spatial resolution. In particular, the spatiotemporal resolution must be faster than the typical rate of walking at the physiological ATP concentration.

We used Fluorescence Imaging with One Nanometer Accuracy (FIONA) (*2*, *9*) to track GFP-labeled peroxisomes being carried by microtubule motors with 1.5 nm accuracy and 1 msec time resolution, inside a live cell, thereby allowing *in vivo* ATP concentrations. We used cultured *Drosophila* S2 cells that constitutively express EGFP with a peroxisome-targeting signal (*10*). Fluorescence images of peroxisomes, excited with total internal epifluorescence microscopy, and labeled with numerous EGFP molecules, can be fit to a Gaussian function, and then well localized (Fig. 1). Figure 1 shows a cell in a bright-field image (treated as described below), a fluorescence image showing the EGFP-peroxisomes, and a 1 msec point-spread-function of one peroxisome, which shows localization to 1.5 nm.

Most organelles use both microtubule motors and myosins for intracellular movement (reviewed in (*11*)). In order to analyze the work of microtubule motors in the absence of myosin effects, we have treated cells with 5 μM of cytochalasin D, a drug that caps barbed ends of actin filaments resulting in disappearance of long filaments and therefore inhibition of actomyosin-dependent movement. Normal S2 cells plated on a substrate coated with concanavalin A have a discoid shape (*12*). Upon the loss of the actin filament network, S2 cells grow thin processes that are filled with microtubules (see e.g. Fig. 1), but have no F-

actin cables detectable by fluorescent phalloidin staining (data not shown). We analyzed the polarity of microtubules in these processes using cells expressing EGFP-tagged EB1 (*12*). EB1 is a protein that specifically binds to plus-ends of growing microtubules (see e.g. (*13*)). We found that in thin processes (diameter ≤ 1 μm) more than 90% of microtubules have (+) ends pointing away from the nucleus (fig. S1). In contrast, in processes with a diameter over 1 μm only about 60% of microtubules have their plus ends pointing away from the cell body, presumably due to a buckling of the microtubules inside the process. Consequently only those peroxisomes moving in processes with a diameter less than 1 μm were analyzed (fig. S1).

Our measurements were performed at 10°C and low temperatures are known to favor microtubule depolymerization, however, immunofluorescent staining with anti-tubulin antibody demonstrated that the incubation at 10°C had no effect on density or distribution of microtubules (fig. S2). We also determined the effect of microtubule lattice movements on peroxisome motion by performing fluorescence recovery after photobleaching experiments on processes containing GFP-tubulin based microtubules. The fluorescence recovery was longer than 1 second, indicating that microtubule lattice movements occur far slower than kinesin and dynein driven organelle movements (fig. S4).

Drosophila S2 cells are highly sensitive to protein knock-down by RNAi (*12*). We used RNAi to find which motors move peroxosomes along microtubules. We tested conventional kinesin (kinesin-1), three members of kinesin-2 family (Klp68D, Klp64D and CG17461), three members of kinesin-3 family (Klp53D, Klp98A, Klp38B) and ncd (a member of kinesin-14 or C-terminal kinesin family), as well as cytoplasmic dynein. We have not been tested depolymerizing kinesins, mitotic kinesins, and kinesins which are not expressed above background level in S2 cells by microarray analysis (*14*). This RNAi analysis shows that organelle transport was inhibited only by RNAi against kinesin-1 and dynein heavy chain, showing that only these motors are responsible for movement (fig. S3).

FIONA localization shows that peroxisomes can move in a step-by-step manner in both anterograde (kinesin) and retrograde (dynein) directions (Fig. 2, A to C). Averaging 169 motor steps, the step size in the kinesin direction was 8.6 ± 2.7 nm (Fig. 3A), and the average speed was 1.5 ± 0.6 μm/sec. In the dynein direction, 188 steps yielded an average of 8.9 ± 2.6 nm (Fig. 3B) and an average speed of 1.7 ± 0.9 μm/sec. The step-size results are in agreement with *in vitro* kinesin and dynein assays (*3*, *5*), which yielded about 8 nm/step. The average speed for dynein (at a saturating ATP concentration) is within a factor of two: 1.7 μm/sec determined here versus 0.7 μm/sec (*4*) or 1.2 μm/sec (*15*). It is within a factor of two to the calculated speed at the maximal rate of *in vitro* ATP hydrolysis by dynein (120 sec^{-1} (*16*)), assuming one hydrolyzed ATP per 8 nm/step. (120 steps/sec x 8 nm/step = 0.96 μm/sec). Finally, the *in vitro* rate for kinesin is 1.0 μm/sec (*4*), compared with 1.5 μm/sec determined here.

Previous optical trap experiments on kinesin show that the bead-motor linkage behaves like an entropic spring (*3*). Based on this fact, if motors of opposite directions were operating simultaneously, then any compliance in the motor stalks would cause a degradation of step sizes, moving in either direction, as one motor took a step while its competitor was also bound to microtubule (fig. S5). We see constant step sizes implying that there is no "tug of war." It appears that motors are somehow regulated, being turned on or off in a fashion where they are not simultaneously dragging the peroxisome. Figure S6 shows that a distribution of the displacement driven by kinesins and dynein showing 8 nm step or multiple of it indicating no degenerated steps by opposite motors.

Figure 3, A and B, show a distribution of speeds for a peroxisome moving in the (+) or (-) directions. The graphs are highly spiked, at intervals corresponding to ≈1.2 μm/sec, extending up to around 12 μm/sec. This implies that they correspond to up to 11 kinesins without dynein creating a significant hindrance (Fig. 3A), or up to 11 dyneins without significant hindrance from kinesin (Fig. 3B). These distinct spikes in speed distributions come from multiple kinesins and multiple dynein which hydrolyzed ATP simultaneously in a stochastic manner., as reducing the cytoplasmic ATP concentration by an ATP-uncoupler FCCP (p-trifluoromethoxy carbonyl cyanide phenyl hydrazone) terminated the fast (>5 μm/sec) organelle transport (data not shown).

In vitro kinesin assays do not show such high velocities: velocities of microtubules gliding on a kinesin coated surface are independent of motor densities with 1-1000 kinesin/μm^2, yielding speeds just above 0.5 μm/sec (*17*). On the other hand, gliding assays done in a more viscous media suggest that at higher loads, the velocity increases at higher motor densities (*18*), suggesting that kinesins can operate together. Other *in vivo* studies show similar fast organelle transport. Ashkin *et al.* have found that mitochondria carried on microtubules can move as fast as 15 μm/sec (*19*). Endosomes in cells can be moved by dynein with speed as fast as 4 μm/sec, faster than *in vitro* dynein speed (*20*). Maximum vesicle velocities in neurons are reported to be 3.5-5 μm/sec, higher than a single microtubule-dependent motor can achieve (*21–24*).

Figure 4 shows traces of individual peroxisomes, which demonstrate that they move at rates greater than the *in vitro* single motor rate. Figure 4A shows one peroxisome moved by dynein at an average rate of 1.0 μm/sec, kinesin then takes

over for two steps, and then dynein takes over again, moving the peroxisome about two times faster than the previous (-) end run (2.2 μm/sec), still in a stepwise manner. Figure 4B shows a peroxisome moved by multiple (perhaps 11) kinesins, then a few dyneins, then kinesins (perhaps 2 in both cases), then multiple dyneins. Figure 4C shows the movement of peroxisome to the (-) end at various speeds over 150 milliseconds. This clearly shows the ability of a peroxisome to be moved by several motors—up to 11 dyneins and 11 kinesins—without any apparent inhibition by the opposite motility partner.

The nature of the coordination is unclear. A small molecule which alternatively turns off kinesin and dynein is one possibility, although it would have to react very quickly to account for a transition time of less than a millisecond between motors. Kinesin and dynein pulling against one another with the stronger one winning, causing the weaker one to uncouple quickly and therefore not creating any load is another possibility. Or perhaps the density and/or flexibility due to the lipid/membrane linkage of motor proteins on the peroxisomes are such that they cannot simultaneously bind to the microtubule. In any case, there has to be a mechanism where the peroxisomes can move by multiple motors much faster than independent, uncoupled, kinesins and dyneins.

In conclusion, our results clearly show that both kinesin and dynein walk with 8 nm steps carrying a real organelle *in vivo*. Faster movements occur with the same step size but with greater rapidity. For the peroxisomes, *in vivo*, up to 11 kinesins or dyneins apparently can work in concert, driving the cargo much faster than seen *in vitro.*

References and Notes

1. R. D. Vale, R. A. Milligan, *Science* **288**, 88 (2000).
2. A. Yildiz, M. Tomishige, R. D. Vale, P. R. Selvin, *Science* **303**, 676 (2004).
3. K. Svoboda, C. F. Schmidt, B. J. Schnapp, S. M. Block, *Nature* **365**, 721 (1993).
4. S. J. King, T. A. Schroer, *Nat Cell Biol* **2**, 20 (2000).
5. R. Mallik, B. C. Carter, S. A. Lex, S. J. King, S. P. Gross, *Nature* **427**, 649 (2004).
6. S. P. Gross, M. A. Welte, S. M. Block, E. F. Wieschaus, *J Cell Biol* **148**, 945 (2000).
7. R. Mallik, S. P. Gross, *Curr Biol* **14**, R971 (2004).
8. S. P. Gross *et al.*, *J Cell Biol* **156**, 855 (2002).
9. A. Yildiz *et al.*, *Science* **300**, 2061 (2003).
10. See supplemental data. For details of measurement see (Yildiz et al, 2003). In terms of microscopy, here we used an Andor Model DV-860 BV, which is a back-illuminated 128 x 128 pixels with 24 uM pixel size, and binned it at 2 x 2 to achieve 1 msec per frame. The cells were kept at 10° C.
11. S. L. Rogers, V. I. Gelfand, *Curr Opin Cell Biol* **12**, 57 (2000).
12. S. L. Rogers, G. C. Rogers, D. J. Sharp, R. D. Vale, *J Cell Biol* **158**, 873 (2002).
13. Y. Ma, D. Shakiryanova, I. Vardya, S. V. Popov, *Curr Biol* **14**, 725 (2004).
14. G. Goshima, R. D. Vale, *J Cell Biol* **162**, 1003 (2003).
15. M. Nishiura *et al.*, *J Biol Chem* **279**, 22799 (2004).
16. T. Kon, M. Nishiura, R. Ohkura, Y. Y. Toyoshima, K. Sutoh, *Biochemistry* **43**, 11266 (2004).
17. R. D. Vale, T. S. Reese, M. P. Sheetz, *Cell* **42**, 39 (1985).
18. A. J. Hunt, F. Gittes, J. Howard, *Biophys J* **67**, 766 (1994).
19. A. Ashkin, K. Schutze, J. M. Dziedzic, U. Euteneuer, M. Schliwa, *Nature* **348**, 346 (1990).
20. M. Lakadamyali, M. J. Rust, H. P. Babcock, X. Zhuang, *Proc Natl Acad Sci U S A* **100**, 9280 (2003).
21. D. B. Hill, M. J. Plaza, K. Bonin, G. Holzwarth, *Eur Biophys J* **33**, 623 (2004).
22. S. T. Brady, R. J. Lasek, R. D. Allen, *Science* **218**, 1129 (1982).
23. B. Grafstein, D. S. Forman, *Physiol. Rev.* **60**, 1167 (1980).
24. C. Kaether, P. Skehel, C. G. Dotti, *Mol Biol Cell* **11**, 1213 (2000).

25. We gratefully acknowledge Ron Vale (UCSF) and Steve Rogers (University of North Carolina at Chapel Hill) for EGFP-EB1 and EGFP-tubulin cell lines. This work supported by NIH grants to P.R.S. (AR44420 and GM 068625) and V.I.G. (GM52111), an NSF grant (to P.R.S.), and the DOE, Division of Material Sciences (under award no. DEFG02-91ER45439) through the Frederick Seitz Materials Research Laboratory at the University of Illinois at Urbana-Champaign (to P.R.S). P.R.S. also thanks Jacquelyn Ackland, Jerome Stenehjem, and the other members of the Sharp Rehabilitation Center of San Diego, for their great care which made this science possible.

Supporting Online Material

www.sciencemag.org/cgi/content/full/1108408/DC1
Materials and Methods
Figs. S1 to S6
References

7 December 2004; accepted 30 March 2005
Published online 7 April 2005; 10.1126/science.1108408
Include this information when citing this paper.

Fig. 1. (**A**) Bright-field image of a cytochalasin-D treated S2 cell with a thin process. (**B**) Fluorescence image of the GFP labeled peroxisomes within the process. (**C**) Fluorescence image of a peroxisome can be fit to a 2D Gaussian (r^2 = 0.992) enabling the center to be determined to 1.5 nm within 1.1 msec.

Fig. 2. Step-by-step movement of peroxisomes carried by (**A**) a single kinesin**,** (**B**) a single dynein, and (**C**) a coordination of kinesin and dynein. (**D**) Histograms of the individual steps of anterograde (kinesin) and retrograde (dynein) movement. A pairwise displacement of kinesin and dynein, showing the multiple of 8 nm displacement is shown in fig. S6.

Fig. 3. (**A** and **B**) Stepping characteristics towards the plus (kinesin) and minus (dynein) ends. Note that in both cases, the graph is highly spiked, apparently corresponding to multiple kinesins (towards the (+) end) or dyneins (towards the (-) end) operating without load from the other motors. Notice in particular, the rapid speed of both dynein and kinesin (up to 12 μm/sec), which is not found in *in vitro* experiments. An event was counted as a contiguous run over 20 nm (see Fig. 4), independent of run length. The runs in the kinesin (+ end) , and in the dynein (- end), directions were counted separately.

Fig. 4. Constant step size but variable speeds. (**A**) A peroxisome takes three steps driven by dynein, then two steps by kinesin, then approximately four steps by two dyneins, based on their average rate of stepping. (**B**) A peroxisome moved by approximately 11 kinesin, then two dyneins, then (one or) two kinesins, then three dyneins. (**C**) A peroxisome driven by dyneins at various speeds. A, B, and C are from different peroxisomes. “m” is their slope

Corrected 12 April 2005

Citations of Fig. 4 were changed to Fig. 3. on page 2, right column.

Citations of Fig. 5 were changed to Fig. 4. on page 2, right column, and page 3, left column.

The notation for retrograde and anterograde was switched on page 2, left column, last paragraph, and in the legend to Fig. 2D on page 4.

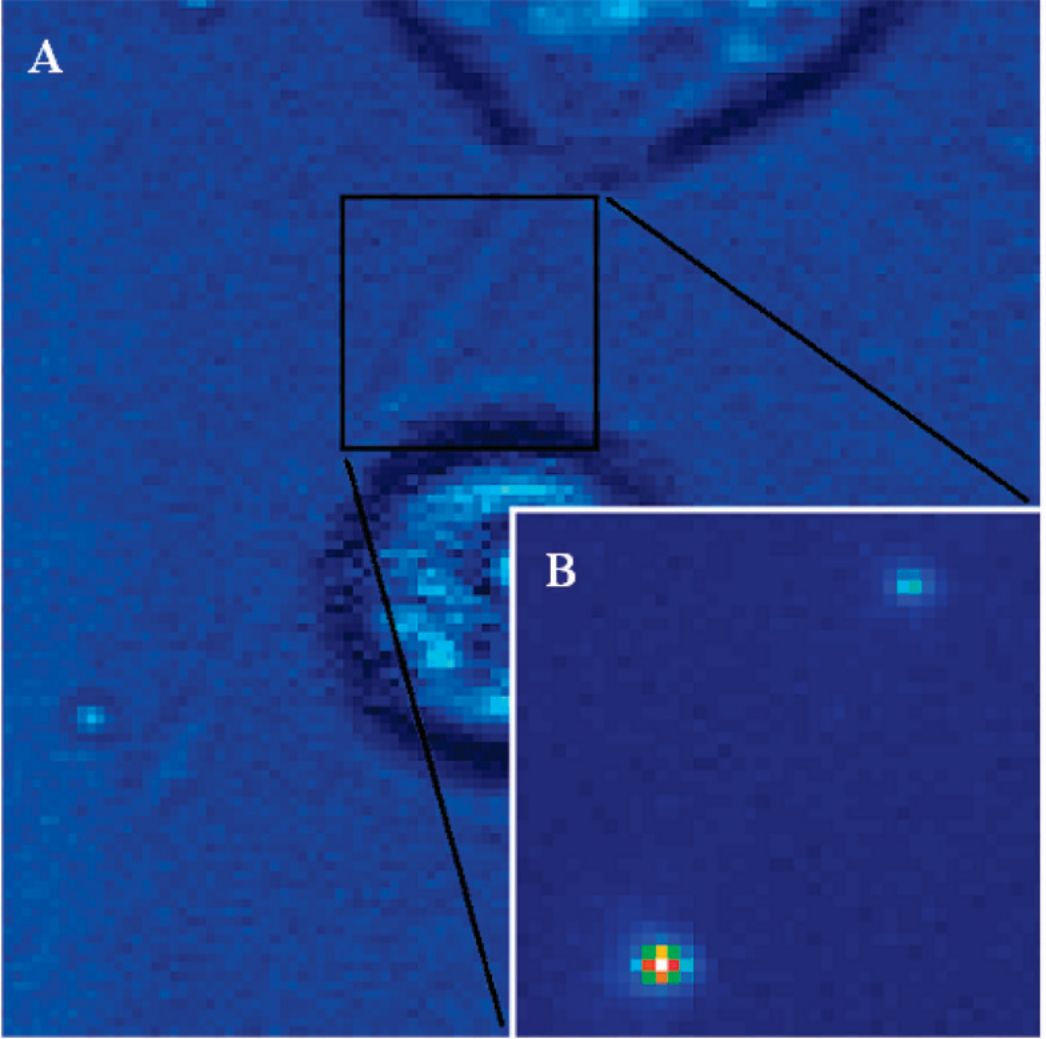
A
B

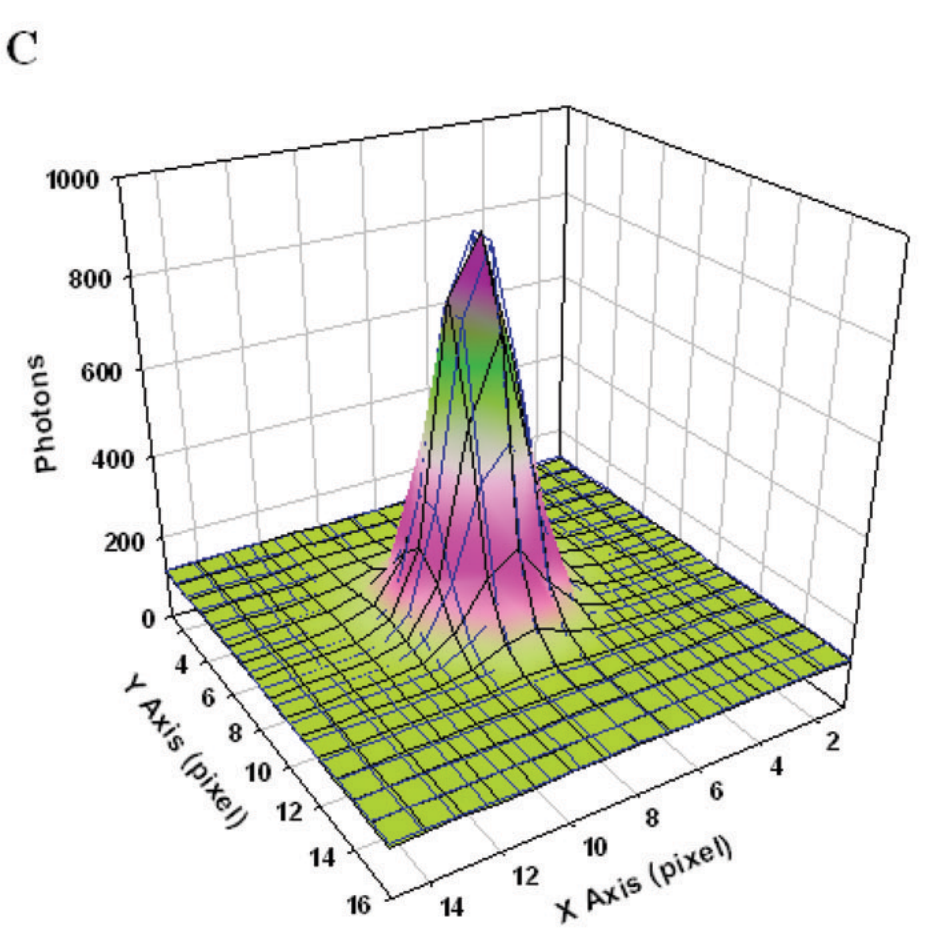
C
1000
800
600
400
200
0
Photons
4
6
8
10
12
14
16
Y Axis (pixel)
14
12
10
8
6
4
2
X Axis (pixel)

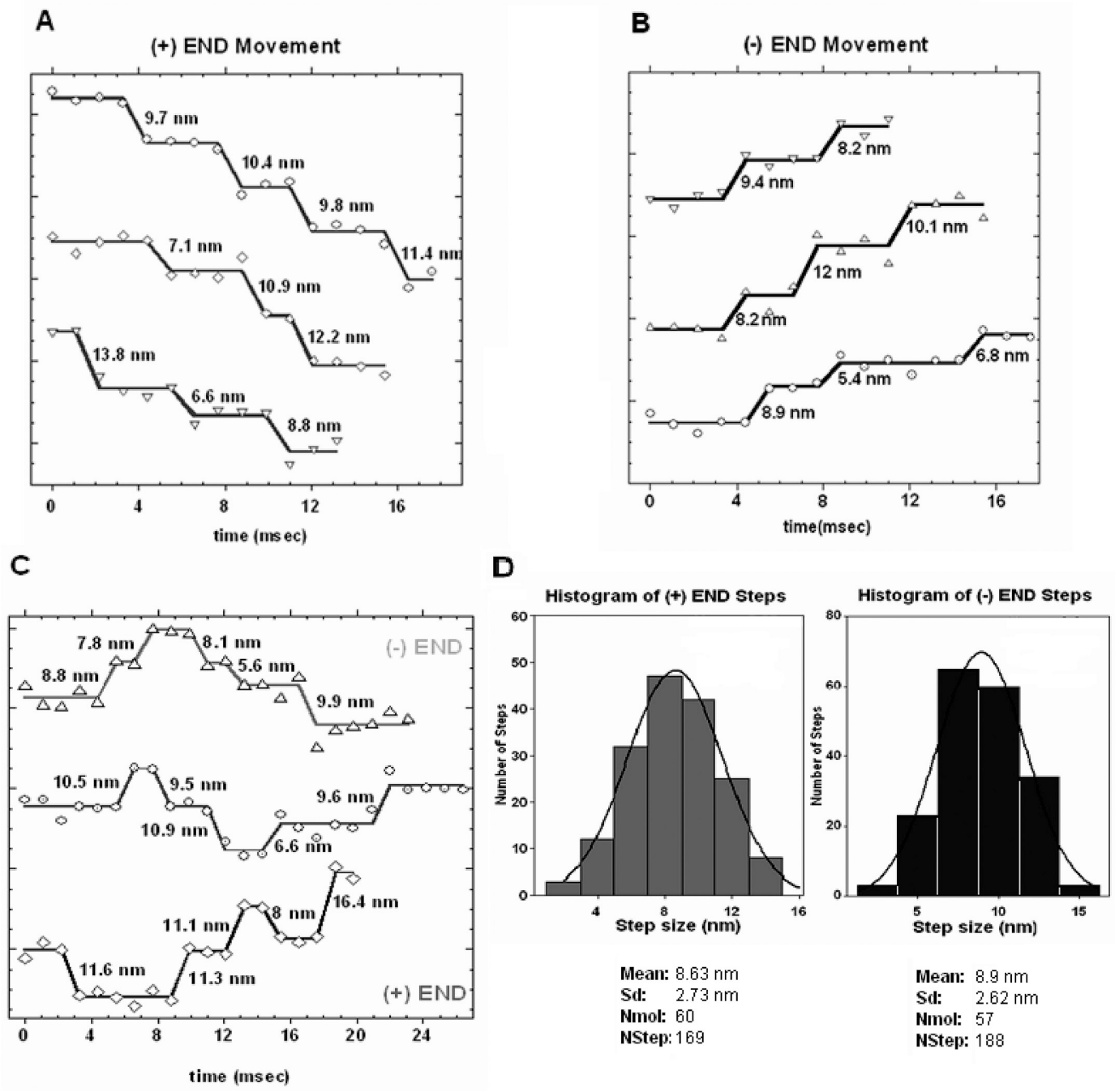
A
(+) END Movement
9.7 nm
10.4 nm
9.8 nm
11.4 nm
7.1 nm
10.9 nm
12.2 nm
13.8 nm
6.6 nm
8.8 nm
0
4
8
12
16
time (msec)
B
(-) END Movement
8.2 nm
9.4 nm
10.1 nm
12 nm
8.2nm
6.8 nm
5.4 nm
8.9 nm
0
4
8
12
16
time(msec)
C
(-) END
7.8 nm
8.1 nm
8.8 nm
5.6 nm
9.9 nm
10.5 nm
9.5 nm
9.6 nm
10.9 nm
6.6 nm
16.4 nm
11.1 nm
8 nm
11.6 nm
11.3 nm
(+) END
0
4
8
12
16
20
24
time (msec)
D
Histogram of (+) END Steps
Number of Steps
Step size (nm)
Mean: 8.63 nm
Sd: 2.73 nm
Nmol: 60
NStep: 169
Histogram of (-) END Steps
Number of Steps
Step size (nm)
Mean: 8.9 nm
Sd: 2.62 nm
Nmol: 57
NStep: 188

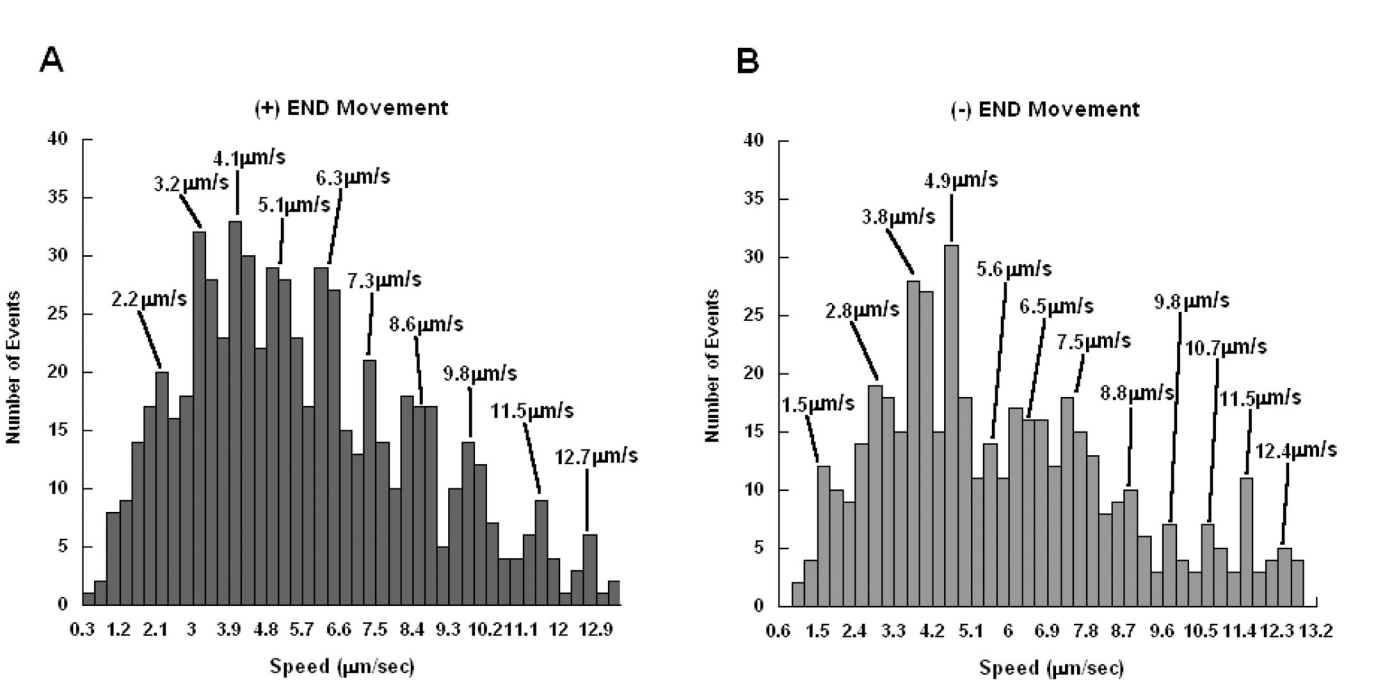
A
(+) END Movement
Number of Events
Speed (μm/sec)
0.3 1.2 2.1 3 3.9 4.8 5.7 6.6 7.5 8.4 9.3 10.2 11.1 12 12.9
2.2μm/s
3.2μm/s
4.1μm/s
5.1μm/s
6.3μm/s
7.3μm/s
8.6μm/s
9.8μm/s
11.5μm/s
12.7μm/s
B
(-) END Movement
Number of Events
Speed (μm/sec)
0.6 1.5 2.4 3.3 4.2 5.1 6 6.9 7.8 8.7 9.6 10.5 11.4 12.3 13.2
1.5μm/s
2.8μm/s
3.8μm/s
4.9μm/s
5.6μm/s
6.5μm/s
7.5μm/s
8.8μm/s
9.8μm/s
10.7μm/s
11.5μm/s
12.4μm/s

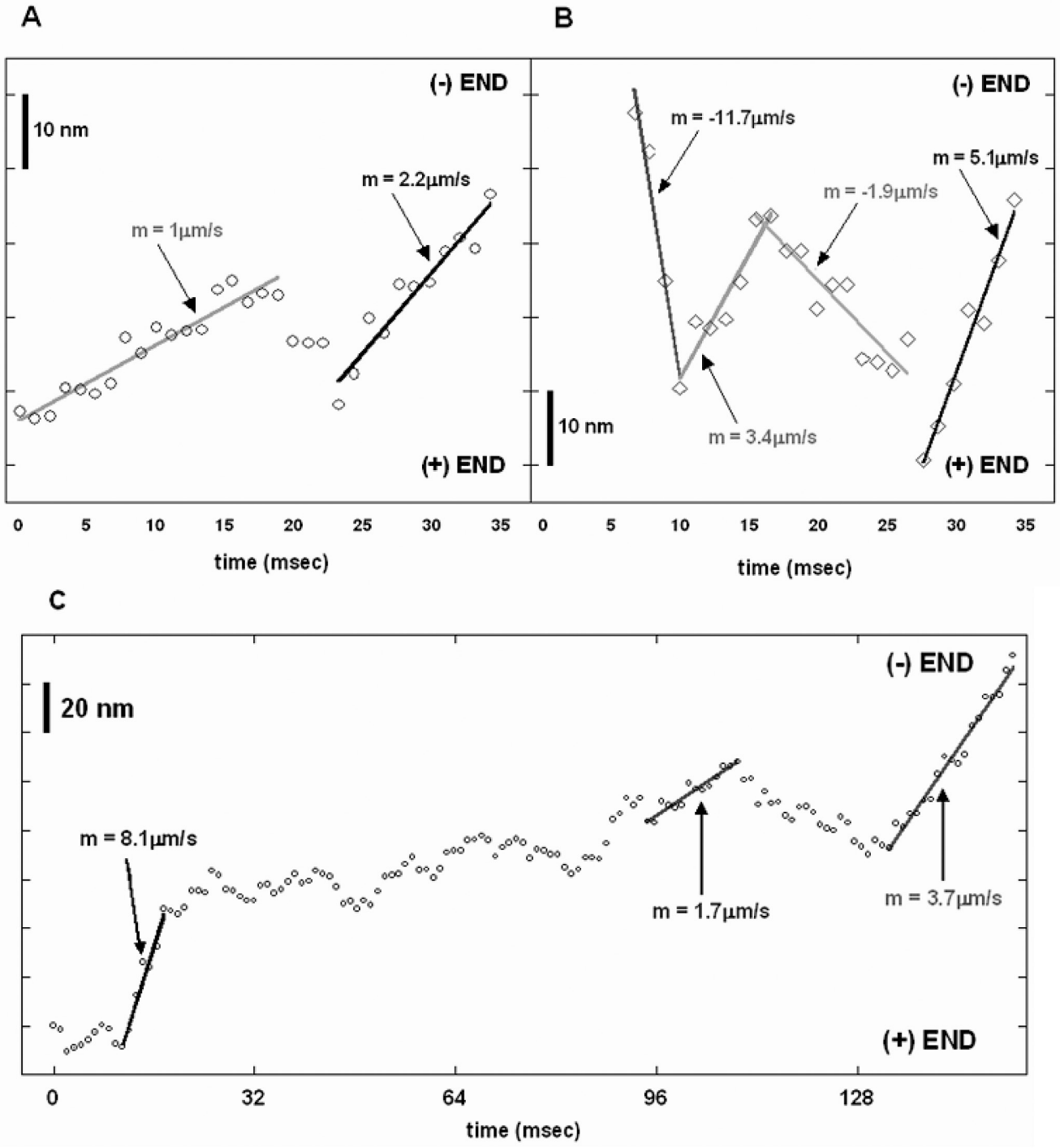
A
B
C
(-) END
(+) END
10 nm
m = 1μm/s
m = 2.2μm/s
m = -11.7μm/s
m = -1.9μm/s
m = 5.1μm/s
m = 3.4μm/s
time (msec)
0
5
10
15
20
25
30
35
20 nm
m = 8.1μm/s
m = 1.7μm/s
m = 3.7μm/s
32
64
96
128